Article

Cell Reports

Excess Synaptojanin 1 Contributes to Place Cell Dysfunction and Memory Deficits in the Aging Hippocampus in Three Types of Alzheimer's Disease

Graphical Abstract

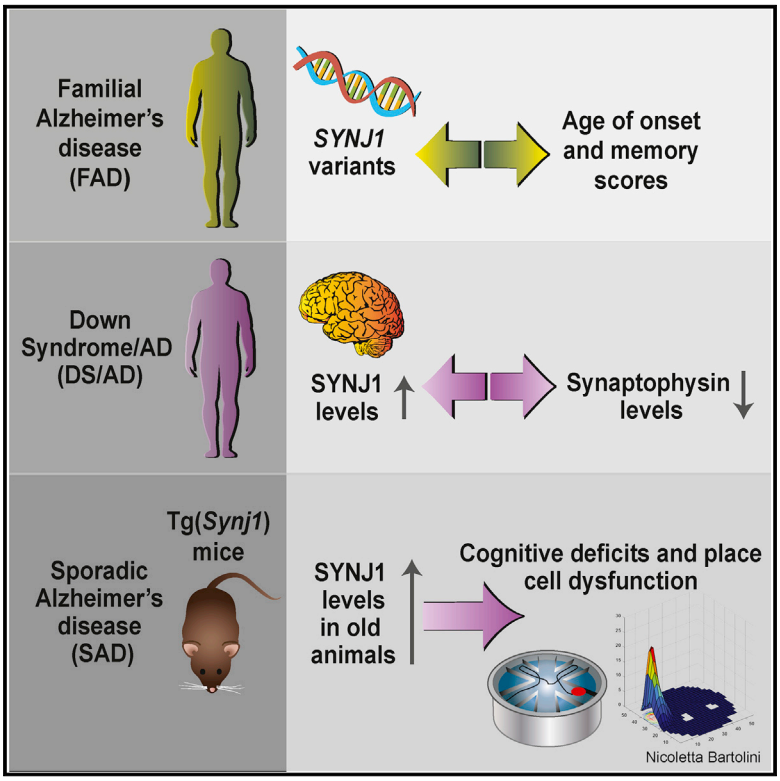

Highlights

- *SYNJ1* variants associate with age of onset in familial Alzheimer's disease
- SYNJ1 and synaptophysin are inversely correlated in adults with Down syndrome
- Aged mice overexpressing Synj1 exhibit cognitive decline and place field defects

Authors

Andre M. Miranda, Mathieu Herman, Rong Cheng, ..., Joseph H. Lee, S. Abid Hussaini, Catherine Marquer

Correspondence

cm3244@cumc.columbia.edu

In Brief

Miranda et al. combine human genetics, human brain samples, and behavior and electrophysiology in a transgenic mouse model to show that synaptojanin 1 levels regulate the function of place cells in the aging hippocampus. The results have implications for memory deficits in all types of Alzheimer's disease.

Miranda et al., 2018, Cell Reports *23*, 2967–2975
June 5, 2018
https://doi.org/10.1016/j.celrep.2018.05.011

CellPress

Cell Reports
Article

Excess Synaptojanin 1 Contributes to Place Cell Dysfunction and Memory Deficits in the Aging Hippocampus in Three Types of Alzheimer's Disease

Andre M. Miranda,[1,2,3,4,16] Mathieu Herman,[1,2,16] Rong Cheng,[1,5,16] Eden Nahmani,[1,2] Geoffrey Barrett,[1,2] Elizabeta Micevska,[1,2] Gaelle Fontaine,[6] Marie-Claude Potier,[6] Elizabeth Head,[7,8] Frederick A. Schmitt,[7,9] Ira T. Lott,[10,11] Ivonne Z. Jiménez-Velázquez,[12] Stylianos E. Antonarakis,[13] Gilbert Di Paolo,[1,2,15] Joseph H. Lee,[1,5,14] S. Abid Hussaini,[1,2] and Catherine Marquer[1,2,17,*]

[1]Taub Institute for Research on Alzheimer's Disease and the Aging Brain, Columbia University Medical Center, New York, NY 10032, USA
[2]Department of Pathology and Cell Biology, Columbia University Medical Center, New York, NY 10032, USA
[3]Life and Health Sciences Research Institute (ICVS), School of Medicine, University of Minho, 4710-057 Braga, Portugal
[4]ICVS/3B's, PT Government Associate Laboratory, 4806-909 Braga/Guimarães, Portugal
[5]G. H. Sergievsky Center, Columbia University Medical Center, New York, NY 10032, USA
[6]Sorbonne Universités, UPMC Univ Paris 06, Inserm U1127, CNRS UMR7225, ICM, 75013 Paris, France
[7]Sanders-Brown Center on Aging, University of Kentucky, Lexington, KY 40536-0230, USA
[8]Department of Pharmacology & Nutritional Sciences, University of Kentucky, Lexington, KY 40506, USA
[9]Department of Neurology, University of Kentucky, Lexington, KY 40506, USA
[10]Department of Physiology, University of Kentucky, Lexington, KY 40506, USA
[11]Department of Pediatrics and Neurology, School of Medicine, University of California, Irvine (UCI), Orange, CA 92668, USA
[12]Department of Internal Medicine, University of Puerto Rico School of Medicine, San Juan, PR, USA
[13]Department of Genetic Medicine and Development, University of Geneva Medical School and University Hospitals of Geneva, 1211 Geneva, Switzerland
[14]Departments of Epidemiology and Neurology, Columbia University Medical Center, New York, NY 10032, USA
[15]Present address: Denali Therapeutics, South San Francisco, CA 94080, USA
[16]These authors contributed equally
[17]Lead Contact
*Correspondence: cm3244@cumc.columbia.edu
https://doi.org/10.1016/j.celrep.2018.05.011

SUMMARY

The phosphoinositide phosphatase synaptojanin 1 (SYNJ1) is a key regulator of synaptic function. We first tested whether *SYNJ1* contributes to phenotypic variations in familial Alzheimer's disease (FAD) and show that *SYNJ1* polymorphisms are associated with age of onset in both early- and late-onset human FAD cohorts. We then interrogated whether SYNJ1 levels could directly affect memory. We show that increased SYNJ1 levels in autopsy brains from adults with Down syndrome (DS/AD) are inversely correlated with synaptophysin levels, a direct readout of synaptic integrity. We further report age-dependent cognitive decline in a mouse model overexpressing murine Synj1 to the levels observed in human sporadic AD, triggered through hippocampal hyperexcitability and defects in the spatial reproducibility of place fields. Taken together, our findings suggest that SYNJ1 contributes to memory deficits in the aging hippocampus in all forms of AD.

INTRODUCTION

Synaptic function is under the rigorous control of phosphoinositide turnover, and phosphatidylinositol-4,5-bisphosphate ($PtdIns[4,5]P_2$) is particularly important in this process (Di Paolo et al., 2004). The $PtdIns(4,5)P_2$ phosphatase synaptojanin 1 (Synj1) is a key regulator of synaptic vesicle endocytosis and reavailability on the pre-synaptic side (Cremona et al., 1999; Kim et al., 2002; Mani et al., 2007; McPherson et al., 1996; Verstreken et al., 2003), while on the post-synaptic side, it controls the endocytosis of α-amino-3-hydroxy-5-methyl-4-isoxazole-propionic acid (AMPA) receptors (Gong and De Camilli, 2008).

A body of literature supports the importance of SYNJ1 in neurodegenerative disorders, including Alzheimer's disease (AD). Clinically, AD is presented with memory loss and spatial disorientation. Neuropathology hallmarks of this disorder include amyloid plaques, composed primarily of Aβ peptides that result from the sequential cleavage of the amyloid precursor protein (APP), and neurofibrillary tangles of hyperphosphorylated Tau (Querfurth and LaFerla, 2010). The three forms of AD—familial AD (FAD), Down syndrome-related AD (DS/AD), and sporadic AD (SAD)—share common clinical and neuropathology signatures. Although early-onset FAD is caused by mutations in the *APP*, *PSEN1*, or *PSEN2* gene (Reitz et al., 2011) and DS/AD is due to triplication of human chromosome 21 (Hsa21) (Antonarakis, 2017; Wiseman et al., 2015), the most potent genetic risk factor for SAD is the ε4 allele of the *APOE* gene (*APOE4*) (Lambert et al., 2013; Strittmatter et al., 1993).

SYNJ1 was reported to be crucial for the enlargement of early endosomes (Cossec et al., 2012), one of the earliest cellular phenotypes associated with AD, observed before amyloid accumulation and cognitive decline (Cataldo et al., 2000). Enlarged

Table 1. Association of SNP within *SYNJ1* Gene with Age at Onset and Memory Scores in a Cohort of Caribbean Hispanic Families with the *PSEN1-G206A* Mutation

		Age at Onset[a]		Global Memory[b]		Long-Term Recall[b]		Delayed Recall[b]	
SNP	Location (bp)	Beta	p Value	Beta	p Value	Beta	p Value	Beta	p Value
21:34004976	34,004,976	−0.77	0.6602	5.90	0.0397[c]	6.81	0.0083[c]	1.04	0.0504
21:34006054:G:T	34,006,054	14.91	0.0094[c]	9.88	0.3092	5.71	0.5150	1.45	0.4203
21:34012999	34,012,999	0.22	0.8909	6.46	0.0137[c]	7.14	0.0024[c]	1.10	0.0230[c]
21:34019201	34,019,201	−16.14	0.0061[c]	7.06	0.5553	6.84	0.5278	3.00	0.1862
21:34041167	34,041,167	−10.23	0.0010[c]	2.94	0.6074	1.23	0.8125	−0.21	0.8402
rs200644223:34057206:ACGGCCGGG:A	34,057,206–34,057,214	−0.98	0.7395	−15.13	0.0004[c]	−11.55	0.0029[c]	−2.14	0.0066[c]
21:34078985	34,078,985	22.46	0.0050[c]	−0.09	0.9939	−4.05	0.7115	2.39	0.2821

See also Figure S2 and Tables S1 and S2 for additional information.

[a]Covariates included AD, sex, *PSEN1-G206A*, education, *APOE4*, and principal components (PC1, PC2, and PC3). Age at onset is defined as age at onset for affected individuals and age at last examination for unaffected individuals (see text for details).

[b]Covariates included age at onset, sex, education, *APOE4*, and principal components (PC1, PC2, and PC3).

[c]$p < 0.05$.

endosomes are present in neurons of *APOE4* carriers (Cataldo et al., 2000) as well as in fibroblasts and lymphocytes from individuals with DS and SAD (Corlier et al., 2015; Cossec et al., 2012). C99, the C-terminal APP fragment resulting from the activity of β-secretase, has been reported to be required for early endosomal enlargement (Jiang et al., 2010). Importantly though, overexpressing *APP* alone is not sufficient to alter endosomal size (Cataldo et al., 2003), and endosomal size is unaffected in *APP* microduplications (Cossec et al., 2012). However, *Synj1* overexpression alone is sufficient to produce enlarged endosomes in the brain of transgenic mice (Cossec et al., 2012), and *SYNJ1* trisomy results in increased endosomal size in cell lines derived from individuals with partial or full trisomy of Hsa21 (Cossec et al., 2012). In addition, SYNJ1 has also been linked to amyloid toxicity. Oligomers of Aβ peptides disrupt PtdIns(4,5)P_2 metabolism in cultured primary cortical neurons, and genetically decreasing Synj1 levels protects from the inhibitory effect of Aβ oligomers on hippocampal long-term potentiation in brain slices (Berman et al., 2008).

A recent study reported that *APOE4* carriers show increased levels of SYNJ1 compared with non-carriers (Zhu et al., 2015). SYNJ1 is encoded by *SYNJ1*, mapping to Hsa21 (Cremona et al., 2000), and is increased in individuals with DS and DS/AD (Arai et al., 2002; Martin et al., 2014). SYNJ1 levels are thus elevated in individuals at high risk for developing SAD and DS/AD, but very little is known on a potential role for synaptojanin 1 in FAD. To our knowledge, only indirect evidence in model systems has currently been published. Specifically, it has been reported that PtdIns(4,5)P_2 metabolism is disrupted in cells expressing FAD-mutant forms of presenilin 1 (Landman et al., 2006), and earlier studies support that genetically decreasing Synj1 levels rescues cognitive deficits in murine models of FAD (McIntire et al., 2012; Zhu et al., 2013), although the mechanisms involved are still controversial.

The present study addresses whether *SYNJ1* is associated with human FAD. It also explores whether elevated levels of SYNJ1 directly affect cognition in an age-dependent manner. Our work, combining human genetics, human autopsy brain samples, and behavior and *in vivo* electrophysiology studies in a transgenic mouse model overexpressing murine Synj1, Tg(*Synj1*) (Voronov et al., 2008), strongly supports that SYNJ1 plays a role in the function of place cells in the aging hippocampus, with critical implications for memory deficits in all three forms of AD and their possible treatment.

RESULTS

Variants of *SYNJ1* Are Associated with Memory Performance in FAD

Individuals with DS/AD (Martin et al., 2014) and *APOE4* carriers (Zhu et al., 2015) show increased levels of SYNJ1. We thus targeted *SYNJ1* as a candidate gene that may contribute to phenotypic variations in FAD. Specifically, we examined whether *SYNJ1* was associated with memory performance and age of onset in early-onset FAD by testing a cohort of Caribbean Hispanic families with the *PSEN1-G206A* mutation (Table S1) (Athan et al., 2001; Lee et al., 2015). Intriguingly, we observed a gene-wise association of *SYNJ1* with age of onset of AD ($p = 0.0195$) and long-term recall performance ($p = 0.0443$) in this cohort (Table S2). Our subsequent SNP analysis within *SYNJ1*, based on whole-genome sequencing (WGS) data, yielded four SNPs that were significantly associated with age of onset ($p < 0.01$; Table 1). Furthermore, we observed three additional SNPs associated with long-term recall scores and global memory scores ($p < 0.05$; Table 1).

We then determined whether the observed effect was present in late-onset FAD, a form of the disease defined by having multiple family members affected with late-onset AD (Romas et al., 2002; Zhao et al., 2013), by extending our study to the EFIGA cohort (Lee et al., 2011; Romas et al., 2002) (Table S1). Because the EFIGA dataset lacked WGS data, we analyzed the candidate *SYNJ1* region (bp 34,004,976–34,078,985) identified from our early-onset FAD results, using seven tagSNPs that were found to be significant from the genome-wide association study (GWAS) dataset available for the EFIGA cohort (Figure S1 and Table S3). Our subsequent sliding-window haplotype

Table 2. Sliding-Window Haplotype Analysis of *SYNJ1* Gene in Late-Onset FAD (EFIGA)

rs11702774	rs2833930	rs2833931	rs10470165	rs17694546	rs2833934	rs2833935		Model 1	Model 2	H1/H1		H1/–		–/–	
A/G[a]	A/G	A/G	G/A	A/C	A/G	G/A	Haplotype	p Value[b]	p Value[c]	Mean	SD	Mean	SD	Mean	SD
Window1							GAA	0.1145	0.1019	67.9	10.5	70.7	9.8	71.2	9.8
	Window2						AAA	0.2072	0.1828	69.8	10.4	71.1	9.8	71.2	9.7
		Window3					AAA	0.0709	0.0580	80.0	1.4	72.4	10.7	71.0	9.8
			Window4				AAG	0.0709	0.0580	80.0	1.4	72.4	10.7	71.0	9.8
				Window5			AGA	0.0418[d]	0.0342[d]	80.0	1.4	72.5	10.7	70.7	9.8
Window1							GAAA	0.1184	0.1059	67.9	10.5	70.7	9.8	71.2	9.8
	Window2						AAAC	0.3410	0.2979	70.4	10.3	71.0	9.8	71.2	9.7
		Window3					AAAG	0.0714	0.0584	80.0	1.4	72.4	10.7	71.0	9.8
			Window4				AAGA	0.0323[d]	0.0256[d]	80.0	1.4	72.4	10.7	70.7	9.8

See also Figure S1 and Tables S1 and S3 for additional information.
[a]A minor allele is presented first.
[b]Covariates for model 1: Alzheimer's disease, sex, education, *APOE4*, principal components (PCs), and genetic relationship matrix (GRM).
[c]Covariates for model 2: similar to model 1 but excludes *APOE4*.
[d]$p < 0.05$.

analysis indicated that window 5 in a 3-mer analysis (bp 34,020,786–34,027,774) and window 4 in a 4-mer approach (bp 34,020,653–34,027,774) were the primary candidates for harboring the variant(s) that contribute to age of onset of AD (Table 2). Furthermore, we observed that carriers of the minor haplotype (AGA or AAGA) were protected against AD, as their age of onset was delayed by 8–10 years on average (Table 2). The effect of *APOE4* on age at onset was not significant. Our findings in human cohorts thus support an association of *SYNJ1* with both early-onset and late-onset FAD.

To determine whether the candidate SNPs we identified in early-onset FAD may affect *SYNJ1* expression in the brain, we examined the expression quantitative trait loci (eQTL) data in the GTEx Portal, restricting our analysis to the tissues in the frontal cortex. In the frontal cortex, we found that, on the basis of 129 tissue samples, rs2833943 located at 34,041,650 bp and rs66528773 located at 34,080,468 bp were differentially expressed ($p = 0.00788771$ for each). Their m values, representing the likelihood of functional relevance, were 0.978 and 0.995, respectively. Interestingly, the set of AD associated SNPs that were identified from early-onset FAD (Table 1) was in linkage disequilibrium with the eQTL identified in the frontal cortex tissues in the GTEx dataset (Figure S2), suggesting that the identified SNPs (or adjacent SNPs) are likely to influence *SYNJ1* expression.

Elevated SYNJ1 Levels Are Associated with Synaptic Deficits in DS/AD

In light of earlier reports that SYNJ1 levels are elevated in individuals at high risk for developing SAD (Zhu et al., 2015) and DS/AD (Martin et al., 2014), our results in human FAD cohorts strongly suggested that SYNJ1 may play a role in all three forms of AD. This motivated us to investigate whether elevated SYNJ1 affects cognition in an age-dependent manner, an AD hallmark. We hypothesized that a large increase in SYNJ1 levels, such as the one observed in populations at high risk for developing DS/AD (+155% compared with age-matched disomic controls) (Martin et al., 2014), could influence synaptic integrity. To test this hypothesis, we used data previously collected on post-mortem brain samples of individuals with DS at different ages (Martin et al., 2014). We focused on the age range of 40–52 years, when most individuals with DS develop AD. For each individual, we plotted the levels of SYNJ1 against the levels of synaptophysin, a pre-synaptic protein that we used as a direct measure of synaptic integrity (Figure 1). Indeed, synaptophysin levels have been extensively and consistently found to be decreased in individuals with AD and DS/AD (e.g., (Downes et al., 2008; Masliah et al., 1989, 1991; Reddy et al., 2005; Terry et al., 1991). We found that levels of SYNJ1 were inversely correlated ($p = 0.0151$, $R^2 = 0.2862$) with levels of synaptophysin; that is, the higher the levels of SYNJ1, the more synaptic integrity was compromised. In contrast, no such correlation ($p = 0.1784$, $R^2 = 0.2790$) was observed in younger individuals with DS (age range 1–39 years), whose SYNJ1 levels are only mildly higher (+36%) than those of disomic controls (Figure S3). Our results thus strongly suggest that elevated levels of SYNJ1 observed in populations at high risk for developing AD could directly affect synaptic structure, function, or both.

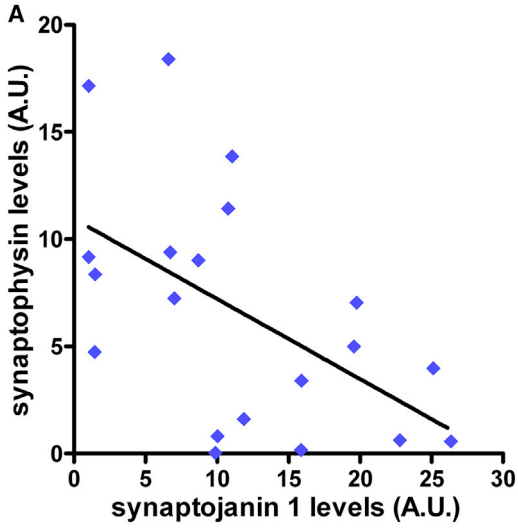

Figure 1. Elevated SYNJ1 Levels Are Associated with Synaptic Deficits in DS/AD

Western blot analysis of SYNJ1 and synaptophysin in human post-mortem brain samples from the mid-frontal cortex (BA46) of individuals with DS, aged 40–52 years (Martin et al., 2014) (n = 20). The line represents the linear regression (R^2 = 0.29, p = 0.015). See also Figure S3 for additional information.

Elevated Synj1 Levels Drive Age-Dependent Hippocampal Cognitive Deficits

To dissect the effect of elevated levels of synaptojanin 1 on cognition, we used a transgenic mouse model overexpressing murine Synj1, Tg(*Synj1*) (Voronov et al., 2008). We observed 76% more Synj1 in the brain of transgenic mice than in littermate controls (wild-type [WT]) (Figure 2A). This closely recapitulates the overexpression levels (+73%) described in *APOE4* carriers with early AD (clinical dementia rating [CDR] 0.5–1) (Zhu et al., 2015) but is milder than the overexpression levels in individuals with DS/AD (+155% compared with age-matched disomic controls) (Martin et al., 2014). Indeed, we found that levels of pre-synaptic (synaptophysin) and post-synaptic (PSD 95) proteins were not altered in the hippocampi of 19-month-old transgenic versus WT animals (Figure S4A), suggesting no gross synaptic loss, even in older animals. Tg(*Synj1*) mice thus appeared as a good model system to dissect the effect of elevated levels of Synj1 on synaptic dysfunction and cognitive deficits.

We focused on two hippocampus-dependent behavior tasks, as this region is critically affected in AD (Stoub et al., 2006), and investigated whether the performance of transgenic Tg(*Synj1*) mice in these tasks declined with age. We first used the radial arm water maze (RAWM) paradigm to probe working memory. At 9 months, Tg(*Synj1*) and WT mice performed similarly in the RAWM test (Figure 2B). In contrast, at 19 months, Tg(*Synj1*) mice showed a significantly higher number of errors in the RAWM compared with WT mice (Figure 2B). Although WT mice experienced cognitive decline with age, age-dependent cognitive deficits were significantly more pronounced in Tg(*Synj1*) than in WT littermates (188% of normal aging; Figure 2C). Although 19-month-old Tg(*Synj1*) swam slightly slower than age-matched WT mice, their ability to reach a visible platform remained unchanged (Figure S4B), ruling out any visual or motivational impairment.

To assess whether other forms of learning were impaired in transgenic mice, we used a fear conditioning (FC) paradigm. Whereas contextual fear learning depends on both hippocampus and amygdala, cued testing only depends on the amygdala. No difference in contextual or cued freezing behavior was observed between Tg(*Synj1*) and WT mice at 9 months (Figure 2D). However, at 19 months, Tg(*Synj1*) mice showed a specific decrease in freezing in contextual but not in cued conditioning compared with WT mice, suggesting hippocampal but not amygdala impairment (Figure 2E). Taken together, our behavior results strongly suggest that increased levels of Synj1 drive age-dependent cognitive deficits in the hippocampus.

Elevated Synj1 Levels Trigger Hippocampal Place Cell Dysfunction

We then pursued the functional basis underlying hippocampal cognitive deficits in older Tg(*Synj1*) animals. Specifically, we investigated whether increased Synj1 levels could alter hippocampal synaptic function using *in vivo* electrophysiological recordings in the hippocampus (Figure S5A). Although the firing of hippocampal inhibitory neurons was not affected (Figure S5B), the average and peak firing rates of hippocampal excitatory neurons were significantly increased in Tg(*Synj1*) mice (+57% and +67% increases compared with WT, respectively; Figure 3A). Because these recorded excitatory neurons were place cells (Hussaini et al., 2011) (Figure 3B), we asked whether place field properties were altered in transgenic animals. The average and peak field firing rates were increased in Tg(*Synj1*) mice compared with WT (Figure 3C). The mean place field size was comparable between transgenic animals and controls (Figure 3D). However, place field size distribution was broader in Tg(*Synj1*) mice, highlighting a higher size variability in transgenic animals (Figure 3D). Information content and spatial coherence were comparable between transgenic and control mice (Figures 3Eand 3F). More important, the stability of place fields after 18–24 hr was decreased by more than 3-fold in Tg(*Synj1*) mice (Figure 3G), suggesting a memory retention deficit.

Overall, our findings indicate that elevated levels of Synj1 trigger acute hyperexcitability as well as dramatic defects in the spatial reproducibility of place fields in the hippocampus of older Tg(*Synj1*) animals. Our data from mouse model systems strongly argue that the elevated levels of SYNJ1 observed in DS/AD and SAD could be the cause of the age-dependent long-term memory defects observed in AD patients.

DISCUSSION

The present study addressed whether the elevated levels of SYNJ1 observed in populations at high risk to develop AD could be a common feature underlying age-dependent cognitive deficits. This study is supported by earlier reports in AD mouse models that described an important role for synaptojanin 1 in mechanisms of neuronal toxicity (Berman et al., 2008; Cossec et al., 2012) and human data that showed elevated levels of SYNJ1 in *APOE4* carriers (Zhu et al., 2015) and in individuals

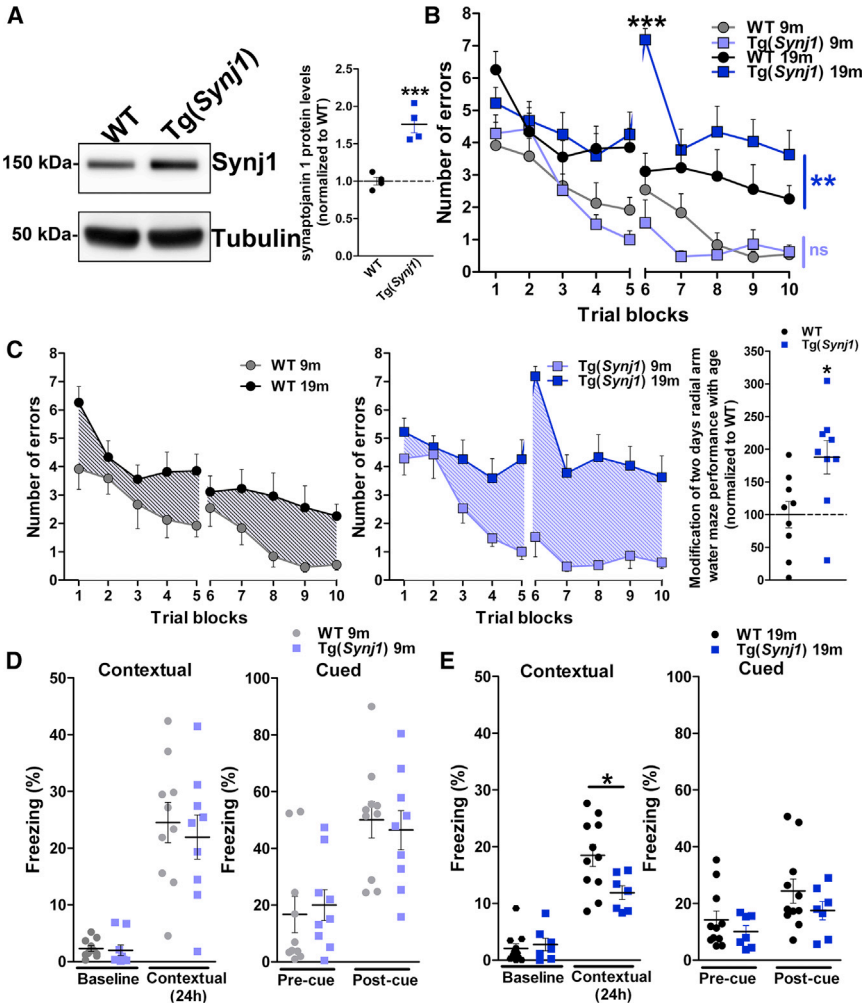

Figure 2. Overexpression of *Synj1* Drives Hippocampal-Dependent Cognitive Deficits in an Age-Dependent Manner

(A) Western blot analysis of Synj1 in 19-month-old WT and Tg(*Synj1*) mice (n = 4). Tubulin was used as an equal loading marker. Synj1 protein levels were 76% higher in Tg(*Synj1*) (1.76 ± 0.11) than in WT (1.00 ± 0.05) mice. ***p < 0.001 in unpaired Student's t test.

(B) Performance of WT and Tg(*Synj1*) mice at 9 (n = 8 WT and 7 Tg[*Synj1*] mice) and 19 (n = 9 mice for both genotypes) months in the radial arm water maze (RAWM). Mice were administered 30 trials over a 2-day period, and the number of errors was averaged over three trials. Two-way ANOVA revealed an interaction between genotype and trial block at 19 months but not at 9 months. ns, p > 0.05, and **p < 0.01 for the overall effect of genotype in two-way ANOVA. In trial 6, ***p < 0.001 for the effect of genotype in two-way ANOVA with Bonferroni post-test.

(C) Age-dependent modification of RAWM performance of WT and Tg(*Synj1*) mice. Age-dependent cognitive deficits were more severe in Tg(*Synj1*) mice (188 ± 25%, n = 9) than in WT mice (100 ± 20%, n = 9). *p < 0.05 in unpaired Student's t test.

(D and E) Freezing response in the contextual and cued FC paradigm in (D) 9-month-old WT (n = 10) and Tg(*Synj1*) (n = 9) mice and in (E) 19-month-old WT (n = 11) and Tg(*Synj1*) (n = 7) mice. *p < 0.05 in unpaired Student's t test.

Data are represented as mean ± SEM. See also Figure S4 for additional information.

with DS/AD (Martin et al., 2014) and answers two previously unaddressed questions. Specifically, this work addresses whether *SYNJ1* is associated with human FAD as well as whether elevated levels of Synj1 directly affect cognition in an age-dependent manner.

Our targeted gene approach extended the relevance of alterations in SYNJ1 to FAD by showing that variants in *SYNJ1* are associated with age of onset and long-term memory deficits in an early-onset FAD cohort of Caribbean Hispanic families with the *PSEN1-G206A* founder mutation. We further showed that variants in *SYNJ1* are also associated with age of onset in the EFIGA cohort of late-onset FAD. Our findings highlight the relevance of studying the impact of SYNJ1 alterations on memory performance for AD. We observed that in DS/AD brain samples, higher SYNJ1 levels correlated with compromised synaptic integrity. We then mimicked milder SYNJ1 overexpression levels, as observed in SAD, in a previously described transgenic mouse model (Voronov et al., 2008). Three- to 4-month-old mice with a mixed FVB/C57BL/6 background showed no anxiety-related behavior (Voronov et al., 2008). They also did not exhibit deficits in the Morris water maze paradigm but performed slightly worse than control animals in the reverse platform test variation of this paradigm (Voronov et al., 2008). For this study, the BAC was backcrossed on the C57BL/6 background for eight generations, and we focused on older, and thus more AD-relevant, animals. Our RAWM and FC behavior studies showed that increased levels of Synj1 triggered age-dependent cognitive deficits in the hippocampus of transgenic Tg(*Synj1*) mice. Our findings support that increased levels of Synj1 did not impair learning per se in older animals, as evident from the non-null slope in trials 1–5 and trials 6–10 in the RAWM, but caused a specific defect in long-term memory retention. This is particularly well illustrated by the very large number of errors in the first trial of day 2 (trial 6; Figure 2B) in the RAWM as well as by the reduced freezing behavior after 24 hr in contextual conditioning (Figure 2E). Using *in vivo* recordings, we showed that this defect is due to hippocampal hyperexcitability and, more specifically, to a dramatic alteration in the spatial reproducibility of hippocampal place fields. Taken together, our data strongly argue that the elevated levels of SYNJ1 observed in populations at high risk to develop AD could be sufficient to trigger age-dependent long-term memory retention impairment, a signature trait of the cognitive deficits observed in AD patients.

A key finding of our study is that levels of synaptojanin 1 can regulate the properties, specifically the spatial reproducibility,

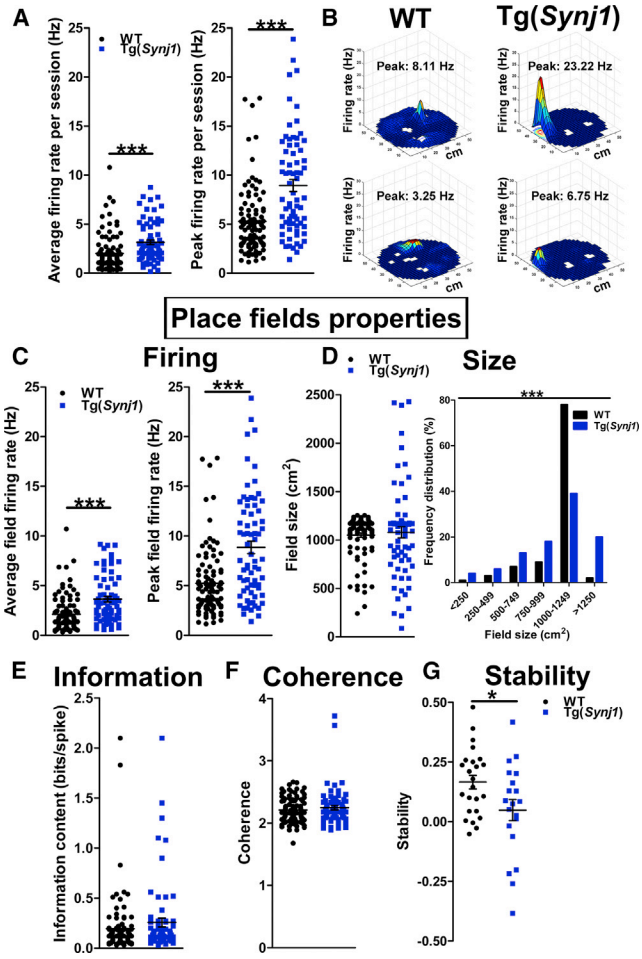

Figure 3. Overexpression of *Synj1* Results in Hippocampal Hyperexcitability and Decreased Place Field Stability

(A) Left: average firing rate of hippocampal excitatory (pyramidal) neurons in 24-month-old Tg(*Synj1*) mice (3.2 ± 0.2 Hz, n = 72 neurons from six animals) and controls (2.0 ± 0.2 Hz, n = 98 neurons from five animals). Right: peak firing rate of pyramidal neurons in Tg(*Synj1*) mice (9.3 ± 0.7 Hz) and controls (5.6 ± 0.4 Hz). ***p < 0.001 in Mann Whitney test.

(B) Representative examples of firing rate maps showing place fields obtained after WT and Tg(*Synj1*) mice explored a 50-cm-diameter cylindrical arena for 20 min. The firing rate is represented by a heatmap ranging from blue (no firing) to red (peak firing). White spaces indicate locations not visited by the animal.

(C) Left: average field firing rate in Tg(*Synj1*) mice (3.8 ± 0.3 Hz, n = 72 neurons) and controls (2.2 ± 0.2 Hz, n = 98 neurons). Right: peak field firing rate in Tg(*Synj1*) mice (9.2 ± 0.7 Hz) and controls (5.5 ± 0.4 Hz). ***p < 0.001 in Mann-Whitney test.

(D) Size of place fields in Tg(*Synj1*) and WT mice. The average size (left) of place fields was comparable (p > 0.05 in Mann-Whitney test) between Tg(*Synj1*) (1,066 ± 58 cm^2, n = 72 neurons) and WT (1,043 ± 24 cm^2, n = 98 neurons) mice, although the distribution (right) of place field sizes was significantly different (***p < 0.001 in chi-square test).

(E) Comparable (p > 0.05, Mann-Whitney test) information content between Tg(*Synj1*) (0.29 ± 0.05 bits/spike, n = 72) and WT (0.19 ± 0.03 bits/spike, n = 98) neurons.

(F) Similar spatial coherence (p > 0.05, Mann-Whitney test) between Tg(*Synj1*) (2.25 ± 0.03, n = 72) and WT (2.21 ± 0.02, n = 98) neurons.

(G) Place field stability at 18–24 hr was significantly decreased (*p < 0.05 in unpaired Student's t test) in Tg(*Synj1*) mice (0.05 ± 0.04, n = 20 neurons) compared with controls (0.17 ± 0.03, n = 24 neurons).

of hippocampal place fields. Indeed, although the unique role of Synj1 in synaptic function has been very well described (Cremona et al., 1999; Gong and De Camilli, 2008; Kim et al., 2002; Mani et al., 2007; Verstreken et al., 2003), how it translates to hippocampal spatial memory encoding remained unknown. This is particularly important in light of the emerging role of SYNJ1 as a crucial regulator in neurodegenerative diseases, including AD and Parkinson's disease. Remarkably, mutations in *SYNJ1* have recently been reported to be associated with early-onset progressive parkinsonism (Kirola et al., 2016; Krebs et al., 2013; Olgiati et al., 2014; Quadri et al., 2013). These mutations affect the role of synaptojanin 1 at the synapse and result in defects in clathrin uncoating (Cao et al., 2017), in autophagosome maturation (Vanhauwaert et al., 2017), or both.

Another central finding highlights the importance of SYNJ1 in AD. Our results establish synaptojanin 1 as a key regulator of age-related cognitive decline and support that modifications of SYNJ1 levels could be a unifying feature of memory deficits observed in the three types of AD (familial, sporadic, and DS/AD). To our knowledge, the only other protein described to be involved in all three forms of AD is APP. Indeed, *APP* can be mutated in FAD, it maps to Hsa21, and variants in the *APP* gene promoter region are a risk factor for SAD (Guyant-Maréchal et al., 2007; Lv et al., 2008).

Our findings thus strongly argue that developing specific SYNJ1 inhibitors is an attractive therapeutic strategy for AD. This is supported by earlier reports showing that genetically decreasing Synj1 levels rescues cognitive deficits in murine models of FAD (*APP* and *PSEN1* mutations) (McIntire et al., 2012; Zhu et al., 2013) and SAD (*ApoE4* knockins) (Zhu et al., 2015). If successful, this therapy would be protective against both toxic effects of oligomeric Aβ (Berman et al., 2008) and cognitive decline linked to age and could be extended to all three forms of AD. Importantly, SYNJ1 can serve as an ideal drug target, as it is a brain-specific phosphatase. That is, its activity can be targeted by small molecules without affecting its structural roles, with limited secondary effects on peripheral organs. Our findings also provide disease-relevant functional readouts, e.g., accuracy of hippocampal spatial encoding, to evaluate the efficacy of these future drugs.

EXPERIMENTAL PROCEDURES

Genetics and Population

Early-Onset FAD

For the genetic study of early-onset FAD, all participating subjects were at least 35 years of age. FAD patients, with the age at onset <65 years, met the research criteria of the National Institute of Neurological and Communicative Disorders and Stroke (NINCDS) and the AD and Related Disorders Association (ADRDA) for probable or possible AD (McKhann et al., 1984). We studied 305 family members from 45 Caribbean Hispanic families that had at least one G206A founder mutation in the *PSEN1* gene (*PSEN1*-G206A), in which approximately 50% of the family members were carriers of the *PSEN1*-G206A (Athan et al., 2001; Lee et al., 2015).

To obtain WGS data on all family members while minimizing sequencing costs, we first selected two to four highly informative family members from each branch of the pedigree using the GIGI algorithm (Cheung et al., 2013)

Data are represented as mean ± SEM. See also Figure S5 for additional information.

and performed WGS on the Illumina HiSeq 2500 platform. In addition, we also performed GWAS on all clinically evaluated family members in the pedigree. To generate WGS data for all family members, we applied SHAPIT2 (Delaneau et al., 2013) and IMPUTE2 (Howie et al., 2009) to impute sequence data into GWAS in family members who were not sequenced. To ensure high-quality imputation in this admixed cohort, we used in-house WGS data generated from 608 Caribbean Hispanics from Puerto Rico and the Dominican Republic, plus the 1000 Genomes data (n = 2,504) as a reference panel. Standard quality control (QC) procedures were performed (Howie et al., 2012). To determine whether genetic variants in *SYNJ1* were associated with variation in age at onset of AD and memory traits, specifically global memory, long-term recall and delayed recall, we first performed a gene-wise analysis while taking into account AD status, sex, *PSEN1*-G206A, level of education, *APOE*4, and principal components 1–3, as implemented in FamSKAT (Chen et al., 2013) for each trait. For the purpose of analysis, we followed the convention of survival analysis and defined age at onset of AD as follows: if affected, age at onset was used as the age at onset; if unaffected, age at last examination was used. To determine whether certain variants within *SYNJ1* were significantly associated with the traits, we performed a SNP-wise analysis for the variants in *SYNJ1* while controlling for the same set of covariates as well as kinship coefficient to take into account non-independence among family members. Linear mixed modeling was performed using R (http://cran.r-project.org/web/packages/kinship2/kinship2.pdf).

Replication in Late-Onset AD

To determine whether the observed genetic association between *SYNJ1* and early-onset FAD was present in late-onset AD as well, we examined the role of SYNJ1 by evaluating the EFIGA cohort, which comprises both Caribbean Hispanic families with late-onset AD (Lee et al., 2011; Romas et al., 2002) and unrelated Caribbean Hispanics with SAD (Tosto et al., 2015) (see Table S1 for their characteristics). Genotyping data were obtained using multiple batches of SNP microarray platforms (see Table S3). We performed a sliding-window haplotype analysis using the GMMAT algorithm (Chen et al., 2016), taking three or four tagSNPs at a time. We then compared the mean age at onset associated with the risk haplotype.

Recruitment, informed consent, and study procedures for the above two studies were approved by the institutional review boards of the Columbia University Medical Center (AAA R5816 for the Genetic modifier study and AAA PO477 for EFIGA).

Human Subjects, Autopsy Brain Tissue, and Western Blot

Characteristics of autopsy cases, as well as brain tissue preparation protocol and western blotting procedures, were previously described in full detail (Martin et al., 2014).

Mouse Models

Two different mouse models were tested: (1) Tg(*Synj1*) mice and (2) their C57BL/6 control littermates (WT). The Tg(*Synj1*) line was a kind gift from the Antonarakis lab. It was generated on the FVB background using mouse BAC RPCI-23 402J16, as described previously (Voronov et al., 2008). This BAC also contains two additional complete genes, the mouse orthologs of *C21orf59* and *C21orf66* (Voronov et al., 2008). The expression of *C21orf59* is enriched in the cerebellum (https://gtexportal.org/home/gene/C21ORF59). The C21orf59 protein controls primary cilia motility and polarization (Austin-Tse et al., 2013; Jaffe et al., 2016). The expression of *C21orf66*, also called *PAXBP1*, is enriched in the cerebellum too (https://gtexportal.org/home/gene/PAXBP1). PAXBP1 is an adaptor protein linking the transcription factors PAX3 and PAX7 to the histone methylation machinery in muscle precursor cells (Diao et al., 2012). A variant of *PAXBP1* was recently linked to myopathic hypotonia (Alharby et al., 2017). Contributing effects from these genes cannot be excluded. For this study, the BAC was backcrossed on the C57BL/6 background for eight generations. Genotypes were assessed using PCR. All animals were hemizygous for the BAC transgene. All procedures were performed following NIH guidelines in accordance with Institutional Animal Care and Use Committee (IACUC) protocols. Tests were performed on 4–14 mice for each genotype group. All experiments were performed blind with respect to the genotype. Behavior experiments were performed on two age groups: 9 months (range 8–11 months) and 19 months (range 18–22 months). Because of technical considerations, *in vivo* electrophysiology recordings were performed on a larger age range (19–31 months), with an average age of 24 months at recording. All experiments were performed on age-matched mice for each genotype group. Separate tests were performed for males and females. Because no sex-specific differences were found, results from both genders were pooled.

Statistical Analysis

Statistical calculations were performed using GraphPad Prism version 5.02. All data are expressed as mean ± SEM. In most cases, when comparing two samples, two-tailed Student's t test was performed. When variances were not comparable, Welch's correction was applied. When the distribution could not be assumed to be Gaussian, we used a non-parametric Mann-Whitney test. When more samples were compared and Bartlett's test showed that variances could be compared, we used one-way ANOVA with Dunnett's post-test or two-way ANOVA with the Bonferroni post-test. If variances could not be compared (p value in Bartlett's test < 0.05), we used t tests. When more samples were compared and when the distribution could not be assumed to be Gaussian, we used the Kruskal-Wallis test. The chi-square test was used to compare distributions. Outliers, defined as values that were superior to (mean + 3 SDs) or inferior to (mean − 3 SDs) were excluded.

DATA AND SOFTWARE AVAILABILITY

The authors declare that all the data supporting the findings of this study are available within the article and its Supplemental Information files or are available from the corresponding author on request. The accession number for the WGS data obtained from members of families with early onset *PSEN1-G206A* mutation carriers reported in this paper is National Institute on Aging Genetics of AD Data Storage Site (NIAGADS): NG00064.

SUPPLEMENTAL INFORMATION

Supplemental Information includes Supplemental Experimental Procedures, five figures, and three tables and can be found with this article online at https://doi.org/10.1016/j.celrep.2018.05.011.

ACKNOWLEDGMENTS

We would like to thank Agnieszka Staniszewski and Dr. Ottavio Arancio for their expert help with behavior studies. We would like to thank Eric Doran and Dr. Sarah B. Martin for their help with DS studies. We want to acknowledge Valerie Savage, Alejandro J. Mercado-Capote, Adithi Jayaraman, and Masayuki Yanagiba for help with microdrive construction and spike sorting. We also want to thank Nicoletta Barolini for her expert help with illustrations and graphics. This work was supported by grants from Fundação para a Ciência e Tecnologia (PD/BD/105915/2014 to A.M.M.), the Philippe Chatrier Foundation (C.M.), the Lejeune Foundation (1149 to G.D.P.), the Alzheimer's Association (2015-NIRG-341570 to S.A.H.), ANR Investissements d'Avenir (ANR-10-IAIHU-06 to M.-C.P.), and the NIH (R01AG050425 to S.A.H.; RO1HD064993 to E.H. and F.A.S.; and RO1HD065160, P50AG16573, and U01AG051412 to I.T.L.). Data collection on Caribbean Hispanic families with at least one G206A founder mutation in the *PSEN1* gene was supported by the BrightFocus Foundation (A2015633S) and NIH/National Institute on Aging (NIA) (R56 AG051876-01A1) to J.H.L. Data collection for the EFIGA project was supported by the Genetic Studies of Alzheimer's Disease in Caribbean Hispanics (EFIGA), funded by the NIH/NIA (5R37AG015473, RF1AG015473, and R56AG051876). We acknowledge the EFIGA study participants and the EFIGA research and support staff for their contributions to this study.

AUTHOR CONTRIBUTIONS

C.M. conceived most of the research. G.D.P. conceived a subset of behavioral experiments. A.M.M., M.H., E.N., E.M., G.F., and C.M. performed experiments. A.M.M., G.B., S.A.H., and C.M. analyzed experiments. R.C. analyzed genetic data from human cohorts. E.H., F.A.S., and I.T.L. contributed key

data on individuals with DS. I.Z.J.-V. played a key role in the recruitment of mutation carriers. S.E.A. contributed a key animal model. M.-C.P., J.H.L., S.A.H., and C.M. supervised the work. C.M., S.A.H., and J.H.L. wrote the manuscript, and all authors critically discussed the data and edited the manuscript.

DECLARATION OF INTERESTS

G.D.P. is a full-time employee of Denali Therapeutics, Inc. All other authors declare no competing interests.

Received: December 18, 2017
Revised: March 1, 2018
Accepted: May 2, 2018
Published: June 5, 2018

REFERENCES

Alharby, E., Albalawi, A.M., Nasir, A., Alhijji, S.A., Mahmood, A., Ramzan, K., Abdusamad, F., Aljohani, A., Abdelsalam, O., Eldardear, A., et al. (2017). A homozygous potentially pathogenic variant in the PAXBP1 gene in a large family with global developmental delay and myopathic hypotonia. Clin. Genet. *92*, 579–586.

Antonarakis, S.E. (2017). Down syndrome and the complexity of genome dosage imbalance. Nat. Rev. Genet. *18*, 147–163.

Arai, Y., Ijuin, T., Takenawa, T., Becker, L.E., and Takashima, S. (2002). Excessive expression of synaptojanin in brains with Down syndrome. Brain Dev. *24*, 67–72.

Athan, E.S., Williamson, J., Ciappa, A., Santana, V., Romas, S.N., Lee, J.H., Rondon, H., Lantigua, R.A., Medrano, M., Torres, M., et al. (2001). A founder mutation in presenilin 1 causing early-onset Alzheimer disease in unrelated Caribbean Hispanic families. JAMA *286*, 2257–2263.

Austin-Tse, C., Halbritter, J., Zariwala, M.A., Gilberti, R.M., Gee, H.Y., Hellman, N., Pathak, N., Liu, Y., Panizzi, J.R., Patel-King, R.S., et al. (2013). Zebrafish ciliopathy screen plus human mutational analysis identifies C21orf59 and CCDC65 defects as causing primary ciliary dyskinesia. Am. J. Hum. Genet. *93*, 672–686.

Berman, D.E., Dall'Armi, C., Voronov, S.V., McIntire, L.B.J., Zhang, H., Moore, A.Z., Staniszewski, A., Arancio, O., Kim, T.W., and Di Paolo, G. (2008). Oligomeric amyloid-beta peptide disrupts phosphatidylinositol-4,5-bisphosphate metabolism. Nat. Neurosci. *11*, 547–554.

Cao, M., Wu, Y., Ashrafi, G., McCartney, A.J., Wheeler, H., Bushong, E.A., Boassa, D., Ellisman, M.H., Ryan, T.A., and De Camilli, P. (2017). Parkinson Sac domain mutation in synaptojanin 1 impairs clathrin uncoating at synapses and triggers dystrophic changes in dopaminergic axons. Neuron *93*, 882–896.e5.

Cataldo, A.M., Peterhoff, C.M., Troncoso, J.C., Gomez-Isla, T., Hyman, B.T., and Nixon, R.A. (2000). Endocytic pathway abnormalities precede amyloid beta deposition in sporadic Alzheimer's disease and Down syndrome: differential effects of APOE genotype and presenilin mutations. Am. J. Pathol. *157*, 277–286.

Cataldo, A.M., Petanceska, S., Peterhoff, C.M., Terio, N.B., Epstein, C.J., Villar, A., Carlson, E.J., Staufenbiel, M., and Nixon, R.A. (2003). App gene dosage modulates endosomal abnormalities of Alzheimer's disease in a segmental trisomy 16 mouse model of down syndrome. J. Neurosci. *23*, 6788–6792.

Chen, H., Meigs, J.B., and Dupuis, J. (2013). Sequence kernel association test for quantitative traits in family samples. Genet. Epidemiol. *37*, 196–204.

Chen, H., Wang, C., Conomos, M.P., Stilp, A.M., Li, Z., Sofer, T., Szpiro, A.A., Chen, W., Brehm, J.M., Celedón, J.C., et al. (2016). Control for population structure and relatedness for binary traits in genetic association studies via logistic mixed models. Am. J. Hum. Genet. *98*, 653–666.

Cheung, C.Y.K., Thompson, E.A., and Wijsman, E.M. (2013). GIGI: an approach to effective imputation of dense genotypes on large pedigrees. Am. J. Hum. Genet. *92*, 504–516.

Corlier, F., Rivals, I., Lagarde, J., Hamelin, L., Corne, H., Dauphinot, L., Ando, K., Cossec, J.C., Fontaine, G., Dorothée, G., et al.; Clinical ImaBio3 Team (2015). Modifications of the endosomal compartment in peripheral blood mononuclear cells and fibroblasts from Alzheimer's disease patients. Transl. Psychiatry *5*, e595.

Cossec, J.C., Lavaur, J., Berman, D.E., Rivals, I., Hoischen, A., Stora, S., Ripoll, C., Mircher, C., Grattau, Y., Olivomarin, J.C., et al. (2012). Trisomy for synaptojanin1 in Down syndrome is functionally linked to the enlargement of early endosomes. Hum. Mol. Genet. *21*, 3156–3172.

Cremona, O., Di Paolo, G., Wenk, M.R., Lüthi, A., Kim, W.T., Takei, K., Daniell, L., Nemoto, Y., Shears, S.B., Flavell, R.A., et al. (1999). Essential role of phosphoinositide metabolism in synaptic vesicle recycling. Cell *99*, 179–188.

Cremona, O., Nimmakayalu, M., Haffner, C., Bray-Ward, P., Ward, D.C., and De Camilli, P. (2000). Assignment of SYNJ1 to human chromosome 21q22.2 and Synj12 to the murine homologous region on chromosome 16C3-4 by in situ hybridization. Cytogenet. Cell Genet. *88*, 89–90.

Delaneau, O., Zagury, J.F., and Marchini, J. (2013). Improved whole-chromosome phasing for disease and population genetic studies. Nat. Methods *10*, 5–6.

Di Paolo, G., Moskowitz, H.S., Gipson, K., Wenk, M.R., Voronov, S., Obayashi, M., Flavell, R., Fitzsimonds, R.M., Ryan, T.A., and De Camilli, P. (2004). Impaired PtdIns(4,5)P2 synthesis in nerve terminals produces defects in synaptic vesicle trafficking. Nature *431*, 415–422.

Diao, Y., Guo, X., Li, Y., Sun, K., Lu, L., Jiang, L., Fu, X., Zhu, H., Sun, H., Wang, H., and Wu, Z. (2012). Pax3/7BP is a Pax7- and Pax3-binding protein that regulates the proliferation of muscle precursor cells by an epigenetic mechanism. Cell Stem Cell *11*, 231–241.

Downes, E.C., Robson, J., Grailly, E., Abdel-All, Z., Xuereb, J., Brayne, C., Holland, A., Honer, W.G., and Mukaetova-Ladinska, E.B. (2008). Loss of synaptophysin and synaptosomal-associated protein 25-kDa (SNAP-25) in elderly Down syndrome individuals. Neuropathol. Appl. Neurobiol. *34*, 12–22.

Gong, L.W., and De Camilli, P. (2008). Regulation of postsynaptic AMPA responses by synaptojanin 1. Proc. Natl. Acad. Sci. U S A *105*, 17561–17566.

Guyant-Maréchal, L., Rovelet-Lecrux, A., Goumidi, L., Cousin, E., Hannequin, D., Raux, G., Penet, C., Ricard, S., Macé, S., Amouyel, P., et al. (2007). Variations in the APP gene promoter region and risk of Alzheimer disease. Neurology *68*, 684–687.

Howie, B.N., Donnelly, P., and Marchini, J. (2009). A flexible and accurate genotype imputation method for the next generation of genome-wide association studies. PLoS Genet. *5*, e1000529.

Howie, B., Fuchsberger, C., Stephens, M., Marchini, J., and Abecasis, G.R. (2012). Fast and accurate genotype imputation in genome-wide association studies through pre-phasing. Nat. Genet. *44*, 955–959.

Hussaini, S.A., Kempadoo, K.A., Thuault, S.J., Siegelbaum, S.A., and Kandel, E.R. (2011). Increased size and stability of CA1 and CA3 place fields in HCN1 knockout mice. Neuron *72*, 643–653.

Jaffe, K.M., Grimes, D.T., Schottenfeld-Roames, J., Werner, M.E., Ku, T.S.J., Kim, S.K., Pelliccia, J.L., Morante, N.F.C., Mitchell, B.J., and Burdine, R.D. (2016). c21orf59/kurly Controls Both Cilia Motility and Polarization. Cell Rep. *14*, 1841–1849.

Jiang, Y., Mullaney, K.A., Peterhoff, C.M., Che, S., Schmidt, S.D., Boyer-Boiteau, A., Ginsberg, S.D., Cataldo, A.M., Mathews, P.M., and Nixon, R.A. (2010). Alzheimer's-related endosome dysfunction in Down syndrome is Abeta-independent but requires APP and is reversed by BACE-1 inhibition. Proc. Natl. Acad. Sci. U S A *107*, 1630–1635.

Kim, W.T., Chang, S., Daniell, L., Cremona, O., Di Paolo, G., and De Camilli, P. (2002). Delayed reentry of recycling vesicles into the fusion-competent synaptic vesicle pool in synaptojanin 1 knockout mice. Proc. Natl. Acad. Sci. U S A *99*, 17143–17148.

Kirola, L., Behari, M., Shishir, C., and Thelma, B.K. (2016). Identification of a novel homozygous mutation Arg459Pro in SYNJ1 gene of an Indian family with autosomal recessive juvenile Parkinsonism. Parkinsonism Relat. Disord. *31*, 124–128.

Krebs, C.E., Karkheiran, S., Powell, J.C., Cao, M., Makarov, V., Darvish, H., Di Paolo, G., Walker, R.H., Shahidi, G.A., Buxbaum, J.D., et al. (2013). The Sac1 domain of SYNJ1 identified mutated in a family with early-onset progressive Parkinsonism with generalized seizures. Hum. Mutat. *34*, 1200–1207.

Lambert, J.C., Ibrahim-Verbaas, C.A., Harold, D., Naj, A.C., Sims, R., Bellenguez, C., DeStafano, A.L., Bis, J.C., Beecham, G.W., Grenier-Boley, B., et al.; European Alzheimer's Disease Initiative (EADI); Genetic and Environmental Risk in Alzheimer's Disease; Alzheimer's Disease Genetic Consortium; Cohorts for Heart and Aging Research in Genomic Epidemiology (2013). Meta-analysis of 74,046 individuals identifies 11 new susceptibility loci for Alzheimer's disease. Nat. Genet. *45*, 1452–1458.

Landman, N., Jeong, S.Y., Shin, S.Y., Voronov, S.V., Serban, G., Kang, M.S., Park, M.K., Di Paolo, G., Chung, S., and Kim, T.W. (2006). Presenilin mutations linked to familial Alzheimer's disease cause an imbalance in phosphatidylinositol 4,5-bisphosphate metabolism. Proc. Natl. Acad. Sci. U S A *103*, 19524–19529.

Lee, J.H., Cheng, R., Barral, S., Reitz, C., Medrano, M., Lantigua, R., Jiménez-Velazquez, I.Z., Rogaeva, E., St George-Hyslop, P.H., and Mayeux, R. (2011). Identification of novel loci for Alzheimer disease and replication of CLU, PICALM, and BIN1 in Caribbean Hispanic individuals. Arch. Neurol. *68*, 320–328.

Lee, J.H., Cheng, R., Vardarajan, B., Lantigua, R., Reyes-Dumeyer, D., Ortmann, W., Graham, R.R., Bhangale, T., Behrens, T.W., Medrano, M., et al. (2015). Genetic modifiers of age at onset in carriers of the G206A mutation in PSEN1 with familial Alzheimer disease among Caribbean Hispanics. JAMA Neurol. *72*, 1043–1051.

Lv, H., Jia, L., and Jia, J. (2008). Promoter polymorphisms which modulate APP expression may increase susceptibility to Alzheimer's disease. Neurobiol. Aging *29*, 194–202.

Mani, M., Lee, S.Y., Lucast, L., Cremona, O., Di Paolo, G., De Camilli, P., and Ryan, T.A. (2007). The dual phosphatase activity of synaptojanin1 is required for both efficient synaptic vesicle endocytosis and reavailability at nerve terminals. Neuron *56*, 1004–1018.

Martin, S.B., Dowling, A.L.S., Lianekhammy, J., Lott, I.T., Doran, E., Murphy, M.P., Beckett, T.L., Schmitt, F.A., and Head, E. (2014). Synaptophysin and synaptojanin-1 in Down syndrome are differentially affected by Alzheimer's disease. J. Alzheimers Dis. *42*, 767–775.

Masliah, E., Terry, R.D., DeTeresa, R.M., and Hansen, L.A. (1989). Immunohistochemical quantification of the synapse-related protein synaptophysin in Alzheimer disease. Neurosci. Lett. *103*, 234–239.

Masliah, E., Terry, R.D., Alford, M., DeTeresa, R., and Hansen, L.A. (1991). Cortical and subcortical patterns of synaptophysinlike immunoreactivity in Alzheimer's disease. Am. J. Pathol. *138*, 235–246.

McIntire, L.B., Berman, D.E., Myaeng, J., Staniszewski, A., Arancio, O., Di Paolo, G., and Kim, T.W. (2012). Reduction of synaptojanin 1 ameliorates synaptic and behavioral impairments in a mouse model of Alzheimer's disease. J. Neurosci. *32*, 15271–15276.

McKhann, G., Drachman, D., Folstein, M., Katzman, R., Price, D., and Stadlan, E.M. (1984). Clinical diagnosis of Alzheimer's disease: report of the NINCDS-ADRDA Work Group under the auspices of Department of Health and Human Services Task Force on Alzheimer's Disease. Neurology *34*, 939–944.

McPherson, P.S., Garcia, E.P., Slepnev, V.I., David, C., Zhang, X., Grabs, D., Sossin, W.S., Bauerfeind, R., Nemoto, Y., and De Camilli, P. (1996). A presynaptic inositol-5-phosphatase. Nature *379*, 353–357.

Olgiati, S., De Rosa, A., Quadri, M., Criscuolo, C., Breedveld, G.J., Picillo, M., Pappatà, S., Quarantelli, M., Barone, P., De Michele, G., and Bonifati, V. (2014). PARK20 caused by SYNJ1 homozygous Arg258Gln mutation in a new Italian family. Neurogenetics *15*, 183–188.

Quadri, M., Fang, M., Picillo, M., Olgiati, S., Breedveld, G.J., Graafland, J., Wu, B., Xu, F., Erro, R., Amboni, M., et al.; International Parkinsonism Genetics Network (2013). Mutation in the SYNJ1 gene associated with autosomal recessive, early-onset Parkinsonism. Hum. Mutat. *34*, 1208–1215.

Querfurth, H.W., and LaFerla, F.M. (2010). Alzheimer's disease. N. Engl. J. Med. *362*, 329–344.

Reddy, P.H., Mani, G., Park, B.S., Jacques, J., Murdoch, G., Whetsell, W., Jr., Kaye, J., and Manczak, M. (2005). Differential loss of synaptic proteins in Alzheimer's disease: implications for synaptic dysfunction. J. Alzheimers Dis. *7*, 103–117, discussion 173–180.

Reitz, C., Brayne, C., and Mayeux, R. (2011). Epidemiology of Alzheimer disease. Nat. Rev. Neurol. *7*, 137–152.

Romas, S.N., Santana, V., Williamson, J., Ciappa, A., Lee, J.H., Rondon, H.Z., Estevez, P., Lantigua, R., Medrano, M., Torres, M., et al. (2002). Familial Alzheimer disease among Caribbean Hispanics: a reexamination of its association with APOE. Arch. Neurol. *59*, 87–91.

Stoub, T.R., deToledo-Morrell, L., Stebbins, G.T., Leurgans, S., Bennett, D.A., and Shah, R.C. (2006). Hippocampal disconnection contributes to memory dysfunction in individuals at risk for Alzheimer's disease. Proc. Natl. Acad. Sci. U S A *103*, 10041–10045.

Strittmatter, W.J., Saunders, A.M., Schmechel, D., Pericak-Vance, M., Enghild, J., Salvesen, G.S., and Roses, A.D. (1993). Apolipoprotein E: high-avidity binding to beta-amyloid and increased frequency of type 4 allele in late-onset familial Alzheimer disease. Proc. Natl. Acad. Sci. U S A *90*, 1977–1981.

Terry, R.D., Masliah, E., Salmon, D.P., Butters, N., DeTeresa, R., Hill, R., Hansen, L.A., and Katzman, R. (1991). Physical basis of cognitive alterations in Alzheimer's disease: synapse loss is the major correlate of cognitive impairment. Ann. Neurol. *30*, 572–580.

Tosto, G., Fu, H., Vardarajan, B.N., Lee, J.H., Cheng, R., Reyes-Dumeyer, D., Lantigua, R., Medrano, M., Jimenez-Velazquez, I.Z., Elkind, M.S.V., et al. (2015). F-box/LRR-repeat protein 7 is genetically associated with Alzheimer's disease. Ann. Clin. Transl. Neurol. *2*, 810–820.

Vanhauwaert, R., Kuenen, S., Masius, R., Bademosi, A., Manetsberger, J., Schoovaerts, N., Bounti, L., Gontcharenko, S., Swerts, J., Vilain, S., et al. (2017). The SAC1 domain in synaptojanin is required for autophagosome maturation at presynaptic terminals. EMBO J. *36*, 1392–1411.

Verstreken, P., Koh, T.W., Schulze, K.L., Zhai, R.G., Hiesinger, P.R., Zhou, Y., Mehta, S.Q., Cao, Y., Roos, J., and Bellen, H.J. (2003). Synaptojanin is recruited by endophilin to promote synaptic vesicle uncoating. Neuron *40*, 733–748.

Voronov, S.V., Frere, S.G., Giovedi, S., Pollina, E.A., Borel, C., Zhang, H., Schmidt, C., Akeson, E.C., Wenk, M.R., Cimasoni, L., et al. (2008). Synaptojanin 1-linked phosphoinositide dyshomeostasis and cognitive deficits in mouse models of Down's syndrome. Proc. Natl. Acad. Sci. U S A *105*, 9415–9420.

Wiseman, F.K., Al-Janabi, T., Hardy, J., Karmiloff-Smith, A., Nizetic, D., Tybulewicz, V.L., Fisher, E.M., and Strydom, A. (2015). A genetic cause of Alzheimer disease: mechanistic insights from Down syndrome. Nat. Rev. Neurosci. *16*, 564–574.

Zhao, W., Marchani, E.E., Cheung, C.Y.K., Steinbart, E.J., Schellenberg, G.D., Bird, T.D., and Wijsman, E.M. (2013). Genome scan in familial late-onset Alzheimer's disease: a locus on chromosome 6 contributes to age-at-onset. Am. J. Med. Genet. B. Neuropsychiatr. Genet. *162B*, 201–212.

Zhu, L., Zhong, M., Zhao, J., Rhee, H., Caesar, I., Knight, E.M., Volpicelli-Daley, L., Bustos, V., Netzer, W., Liu, L., et al. (2013). Reduction of synaptojanin 1 accelerates Aβ clearance and attenuates cognitive deterioration in an Alzheimer mouse model. J. Biol. Chem. *288*, 32050–32063.

Zhu, L., Zhong, M., Elder, G.A., Sano, M., Holtzman, D.M., Gandy, S., Cardozo, C., Haroutunian, V., Robakis, N.K., and Cai, D. (2015). Phospholipid dysregulation contributes to ApoE4-associated cognitive deficits in Alzheimer's disease pathogenesis. Proc. Natl. Acad. Sci. U S A *112*, 11965–11970.

Cell Reports, Volume *23*

Supplemental Information

Excess Synaptojanin 1 Contributes to Place Cell Dysfunction and Memory Deficits in the Aging Hippocampus in Three Types of Alzheimer's Disease

Andre M. Miranda, Mathieu Herman, Rong Cheng, Eden Nahmani, Geoffrey Barrett, Elizabeta Micevska, Gaelle Fontaine, Marie-Claude Potier, Elizabeth Head, Frederick A. Schmitt, Ira T. Lott, Ivonne Z. Jiménez-Velázquez, Stylianos E. Antonarakis, Gilbert Di Paolo, Joseph H. Lee, S. Abid Hussaini, and Catherine Marquer

SUPPLEMENTAL FIGURES AND TABLES

Figure S1. Linkage disequilibrium pattern within a haplotype block generated from the familial late onset AD cohort (EFIGA) using SNPs with p-value <0.05, Related to Table 2. Default parameters in Haploview (Barrett et al., 2005) were used.

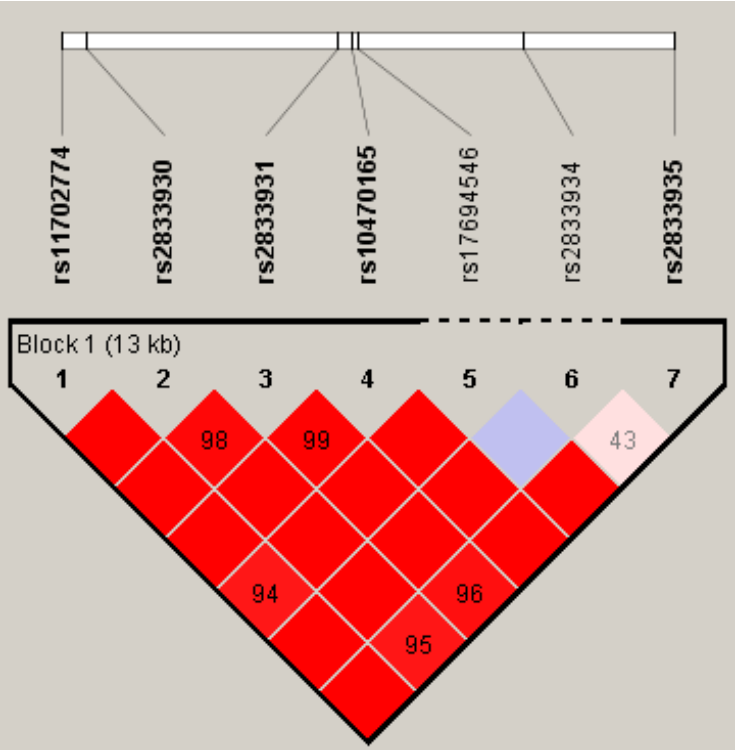

Figure S2. The SNPs identified in *SYNJ1* in the association analysis (Table 1, orange bars) are in linkage disequilibrium (LD) with the eQTLs identified in the GTEx dataset (blue bars), Related to Table 1. In the top part of the figure, the Y1 axis (left, histogram) represent –log p value for genetic association; while the Y2 axis (right, red dots) represent m-values for functional relevance. The linkage disequilibrium (D') patterns between pairwise SNPs were generated using HAPLOVIEW and are presented in the bottom part of the figure. Red squares represent statistically significant LDs; while blue squares represent strong, but not statistically significant, LDs due to small sample size. White squares represent low non-significant LDs.

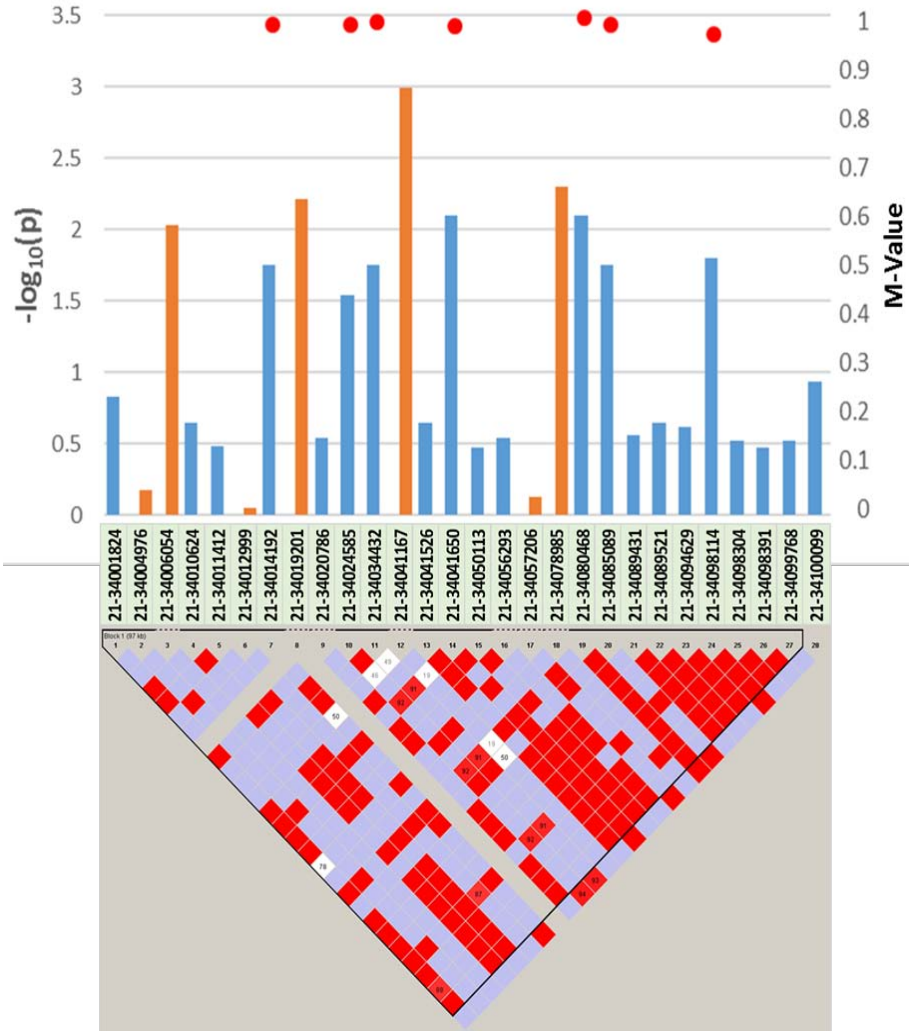

Figure S3. No correlation between SYNJ1 levels and synaptophysin levels in young individuals with DS, Related to Figure 1. Western blot analysis of SYNJ1 and synaptophysin in human post-mortem brain samples from the mid-frontal cortex (BA46) of individuals with DS, aged 1-39 years old (Martin et al., 2014) (n=8). Within this age range, SYNJ1 levels are mildly higher in the DS population (136±47%, n=8), compared to disomic controls (100±12%, n=13), but this difference does not reach significance ($p>0.05$, Student's t-test) (Martin et al., 2014). The line represents the linear regression ($R^2 = 0.28$, $p = 0.178$).

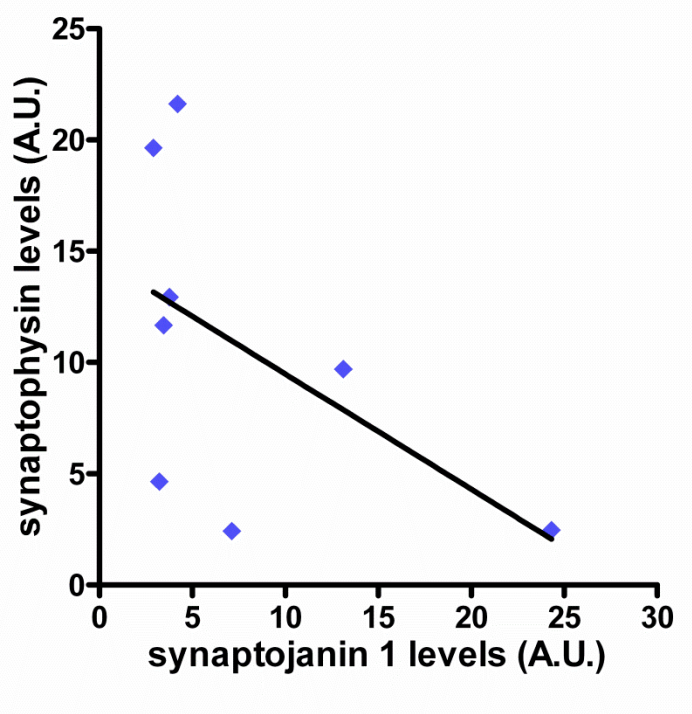

Figure S4. Over-expression of *Synj1* does not affect synaptic protein levels, nor the ability to reach a visible platform, even in older animals, Related to Figure 2. Values denote mean ± S.E.M. (A) Western blot analysis of synaptophysin (SYN) and PSD95 in 19 month-old WT and Tg(*Synj1*) mice (n=4). Tubulin was used as an equal loading marker. Levels of synaptophysin and PSD95 were similar in both genotypes ($p>0.05$ in Student's t-test). (B) Swimming speed (left panel) and latency (right panel) to a visible platform of WT and Tg(*Synj1*) mice. Mice are the same as in Figure 2B and 2C. * denotes $p<0.05$ for the effect of genotype as assessed by two-way ANOVA.

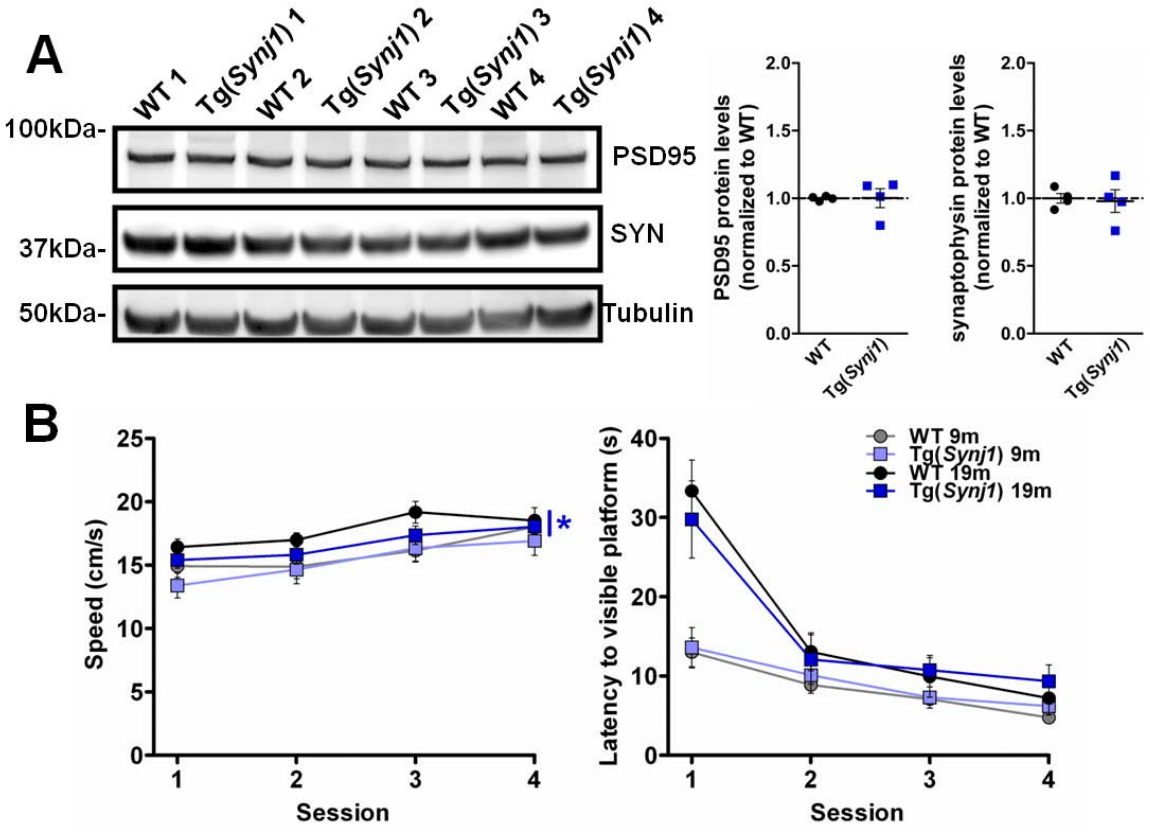

Figure S5. Over-expression of *Synj1* does not affect the firing of inhibitory neurons in the hippocampus, Related to Figure 3. (a) Cresyl violet stained sagittal sections from WT (top) and Tg(*Synj1*) (bottom) animals. Red arrows show electrode trajectories into the hippocampus. (b) Left, the average firing rate of hippocampal interneurons was not significantly altered ($p>0.05$ in Mann Whitney test) in Tg(*Synj1*) (3.4±0.5 Hz, n=36 neurons from 6 animals), compared to controls (4.9±1.1 Hz, n=19 neurons from 5 animals). Right, the peak firing rate of hippocampal interneurons was not significantly altered ($p>0.05$ in Mann Whitney test) in Tg(*Synj1*) (8.2±0.8 Hz, n=36 neurons from 6 animals), compared to controls (9.8±1.6 Hz, n=19 neurons from 5 animals).

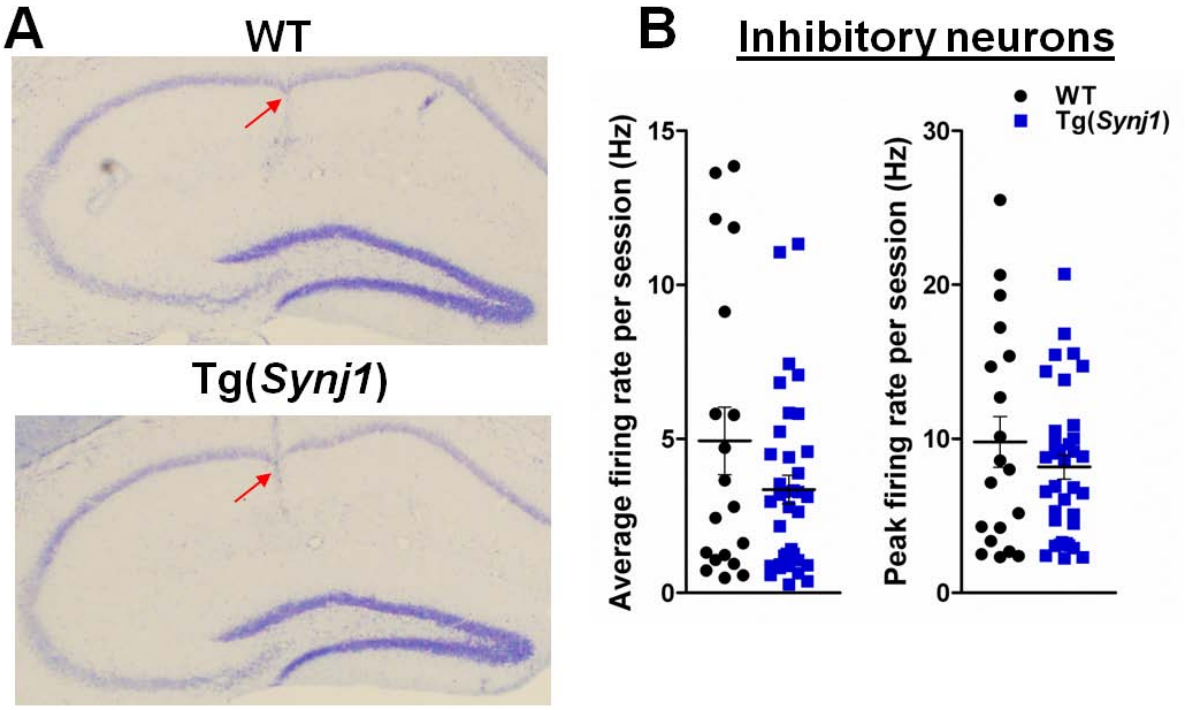

Table S1, Clinical and demographic characteristics of the participating families and their members, Related to Tables 1 and 2. EOAD: early-onset Alzheimer's disease; LOAD: late-onset Alzheimer's disease.

Characteristics	**EOAD**		**LOAD (EFIGA)**	
	Genotyped		**Genotyped**	
	n	**Mean/%**	**n**	**Mean/%**
Familial AD				
Number of families	45		546	
Number of subjects genotyped	305		2199	
Sporadic AD				
Hispanic Sporadic Cases			983	
Hispanic Controls			843	
Affection status				
Affected	74	24.3%	2058	51.1%
Unaffected	231	75.7%	1967	48.9%
Proportion of males: females	132:173	43.3:56.7	1383:2642	34.4:65.6
Age				
Age at onset age (affected)		54.7±7.8		74.4±9.1
Age at last examination (unaffected)		55.5±11.4		67.5±9.3
APOE frequency				
E4	99	16.2%	2206	25.0%
E3	481	78.9%	6216	69.9%
E2	30	4.9%	446	5.1%
G206A Mutation Status				
Carrier	146	47.9%	NA	NA
Non-Carrier	153	50.2%	NA	NA
Unknown	6	2.0%	NA	NA
Education (years)				
Affected	74	11.3±4.5	2058	4.4±4.4
Unaffected	213	12.8±3.8	1967	8.4±5.7
Global Memory (Memory 1)				
Affected	70	8.9±11.4	2058	11.0±10.7
Unaffected	231	34.7±15.4	1967	36.4±9.3
Long-term recall (Memory 2)				
Affected	70	3.4±6.8	2058	5.0±6.4
Unaffected	231	24.0±14.6	1967	24.4±10.7
Delayed recall (Memory 3)				
Affected	70	0.6±1.3	2048	0.9±1.4
Unaffected	230	5.0±3.0	1964	4.8±2.2

Table S2. Gene-wise association analysis for 4 AD-related quantitative traits, Related to Table 1. Bold indicates p<0.05.

Phenotype	N	Number of variants examined in SYNJ1	p-value
Age at onset [(a)]	263	502	**0.0195**
Global memory [(b)]	273	503	0.21499
Long-term recall [(b)]	273	503	**0.04429**
Delayed recall [(b)]	272	500	0.67878

[a] For the age at onset trait, covariates included AD, sex, *PSEN1*-G206A, education, *APOE*4, and principal components (PC1, PC2 and PC3). See text for the definition of age at onset.

[b] For the three memory traits, covariates included age at onset, sex, *PSEN1*-G206A, education, *APOE*4, and principal components (PC1, PC2 and PC3).

Table S3. Multiple genotyping platforms used for the Hispanic GWAS study, Related to Table 2.

STUDY	Microarray SNP chips
Batch 1	Illumina 660k
Batch 2	Illumina 1M
Batch 3	Illumina Omni Express
Batch 4	Infinium OmniExpress
Batch 6	Infinium Global Screening Array
Puerto Rico	Infinium Global Screening Array

SUPPLEMENTAL EXPERIMENTAL PROCEDURES

Differential gene expression in GTEx.

To determine whether variants in *SYNJ1* affect its expression in the brain, we examined the eQTL data (Release V7 (dbGaP Accession phs000424.v7.p2) in the GTEx Portal (https://www.gtexportal.org), restricting our analysis to the 129 tissues in the frontal cortex (BA9) (age range: 20-79 years). Using all variants located within the gene plus those located within 1 MB on either side of the gene, eQTL analysis was performed using the FastQTL algorithm (Ongen et al., 2016), which examines expression levels as a function of SNP dosage, genotype-based principal components, and probabilistic estimation of expression residuals (PEER) (Stegle et al., 2012).

Radial Arm Water Maze (RAWM)

RAWM was performed as described previously (Alamed et al., 2006; McIntire et al., 2012). Briefly, the system consisted of a steel white tank filled with milky water, and containing white walls positioned to produce six arms, radiating from a central area. Spatial cues were present on the walls of the testing room. The location, at the end of one of the arms, of a clear 10 cm plexiglas submerged platform, remained the same for each mouse for the whole duration of the test. On each trial, the mouse started the task from a different randomly chosen arm. Each trial lasted 1 min and errors were counted each time the mouse entered the wrong arm with four paws, or did not take any decision regarding which arm to explore within 10 seconds**.** Each mouse was tested for 15 trials each day for two consecutive days. On the first day, mice were trained for 15 trials, with the first 12 trials alternating between visible (flagged) and hidden (submerged) platform. The last 3 trials of the first day and all of the 15 trials of the second day were performed with a

submerged platform. Results were analyzed by dividing the 30 trials into 10 trial blocks and calculating the average error for each trial block. Tests were performed on 7-9 age-matched mice for each genotype group. All experiments were performed blind with respect to the genotype. Separate tests were performed for males and females. Because no sex-specific differences were found, results from both genders were pooled. Modification of performance with age was quantified by measuring the area under the curve (AUC) for each animal and subtracting [the average AUC for all animals of a given genotype at 9 months] from [the AUC for individual 19 month-old animal of this genotype]. All results were normalized to WT.

Visible platform test

After completing the RAWM experiments, we performed visible platform tests to detect any visual, motor or motivational impairment. These tests were carried out in the same pool but without arms and with a visible (flagged) platform. The platform location was randomly modified to eliminate any contribution of external spatial cues. Mice were given two sessions of three trials each day over 2 days. Each animal was allowed to swim for 1 min from a random location. The time taken (latency) and speed (velocity) to reach the platform were recorded and analyzed using a ceiling-mounted camera, an HVS- 2020 video tracking system and the EthoVision software. Failure to reach the platform was scored as 60 s. Results were analyzed by dividing the 12 trials into 4 trial blocks and calculating an average value for each trial block.

Fear conditioning (FC)

In this paradigm, an innocuous conditioned stimulus (CS), a tone, elicits fear response after being associatively paired with an aversive unconditioned stimulus (US), a foot

shock. The fear response was measured by the frequency of freezing behaviors, which is defined as a stereotyped motionless crouching posture. Contextual and cued FC were performed in a conditioning chamber as previously described (McIntire et al., 2012). Briefly, mice were placed in the conditioning chamber for 2 min before the onset of a discrete tone (CS) (a 30 s sound at 2800 Hz and 85 dB). In the last 2 s of the CS, mice were given a foot shock (US) of 0.50 mA for 2 s through the bars of the floor. After the CS/US pairing, the mice were left in the conditioning chamber for another 30 s and then placed back in their home cages. Freezing behavior was scored using EthoVision software. To evaluate contextual fear learning, freezing was measured for 5 min in the chamber in which the mice were trained 24 hr before the test. To evaluate cued fear conditioning, following contextual testing, the mice were placed in a novel context (cage with smooth flat floor and with vanilla odorant) for 2 min (pre-CS test), after which they were exposed to the CS for 3 min (CS test), and freezing was measured. Tests were performed on 6-14 age-matched mice for each genotype group. All experiments were performed blind with respect to the genotype. Separate tests were performed for males and females. Because no sex-specific differences were found, results from both genders were pooled.

Murine brain tissue preparation and western blot

Mice were anesthetized with ketamine and xylazine (100 and 10 $mg.ml^{-1}$, respectively) and transcardially perfused with saline. Hippocampi were dissected, flash-frozen in liquid nitrogen and kept at -80°C for western blot analysis. Frozen regions were weighed and homogenized in 10 volumes of RIPA buffer (Thermo Fisher) using a microtube homogenizer (VWR). The resulting suspension was then centrifuged at 16,000 g for 15

min. Total protein content was estimated with BCA Protein assay kit (Thermo Fisher). Normalized samples, with the exception of the ones used for synaptojanin 1, were boiled for 10 min at 95 °C in 2x LDS sample buffer (Thermo Fisher) and 10x Sample Reducing Agent (Thermo Fisher). SDS–PAGE was performed on samples (30 μg total proteins) loaded in NuPAGE 4–12% Bis-Tris gels (Thermo Fisher). Wet transfer was performed at 80V for 105 min at 4 °C in Tris-glycine 0.5%-SDS (Boston Bioproducts). Primary and secondary antibodies were incubated overnight at 4 °C and 60 min at room temperature, respectively. Western blot analysis was performed with antibodies raised against Synaptojanin 1 (1:5000, 145 003, SynapticSystems), PSD95 (1:2,000, 51-6900, Thermo Fisher) and synaptophysin (1:2,000, SY38, Millipore). Tubulin (1:10,000, T5168, Sigma) was used for normalization. Peroxidase-conjugated secondary antibodies were from Biorad and were used at a dilution of 1:3,000 (1:10,000 for tubulin). Revelation was performed with Immobilon Western Chemiluminescent HRP Substrate (EMD Millipore) and the chemiluminescent signal was imaged with ImageQuant LAS4000 mini (GE Healthcare). Quantification was performed with ImageJ. At least 4 mice of each genotype were used and each group was gender-matched.

Electrode implantation and surgery

Custom-made, reusable 16-channel microdrives (Axona, UK) were constructed as described previously (Hussaini et al., 2011) by attaching an inner (23 ga) and an outer (19 ga) stainless steel cannula to the microdrives. Tetrodes were built by twisting four 25 mm thick platinum-iridium wires (California wires) and heat bonding them. Four such tetrodes were inserted into the inner cannula of the microdrive and connected to the wires of the microdrive. One day prior to surgery, tetrodes were cut to an appropriate length

and plated with a platinum solution until the impedance dropped to about 150 kOhms. On the day of surgery, mice were anesthetized with either a mixture of ketamine (100 mg/kg) and xylazine (10 mg/kg) or with 1-5% isoflurane mixed with oxygen. Mice were then fixed within the stereotaxic frame with the use of zygomatic process cuff holders. An incision was made to expose the skull and about 3-4 jeweler's screws were inserted into the skull to support the microdrive implant. An additional screw connected with wire was also inserted into the skull and served as a ground/reference for EEG recordings. A 2 mm hole was made on the skull at coordinates 1.8 mm ML and 1.8 AP from bregma. Tetrodes were then lowered to about 0.9 mm from the surface of the brain. Dental cement was spread across the exposed skull and secured with the microdrive. Mice were allowed to recover from anesthesia in a clean cage placed on a warm heating pad until awake (~15 min) before being transported to housing. Carprofen (5 mg/kg) was administered to mice prior to surgery and post-operatively to reduce pain. Mice usually recovered within 24 h, after which the tetrodes were lowered and recording begun. Both male and female mice were used. At least five 24-month old mice of each genotype were used.

In vivo recording and place cell analysis

Mice explored a white box (50 x 50 cm) or a white cylinder (dia. 50 cm). All mice underwent two recording sessions of 10-20 minutes per day, with ≥ 4 hr between sessions. Only sessions with similar coverage (>30%) were analyzed across groups. Tetrode positions were not moved more than 50 μm at a time, and only after the last recording session of the day, allowing > 12 hr of stable electrode positioning prior to the next recording session. All mice included in our study underwent ≥ 16 recording sessions. Neuronal signals from experimental mice were recorded using the Axona

DaqUSB system. Signals were amplified 15,000 to 30,000 times and band-pass filtered between 0.8 and 6.7 kHz. EEG was recorded from 4 channels of the electrodes. EEG was amplified 15,000 times, low-pass filtered at 500 Hz and sampled at 4,800 Hz. Notch filter was used to eliminate 60 Hz noise. The recording system tracked the position of the infrared LED on the head stage (sampling rate 50 Hz) by means of an overhead video camera. Position data were speed-filtered and only speeds of 3 cm/s or more were included. Tracking artifacts were removed by deleting samples greater than 100 cm/s and missing positions were interpolated with total durations less than 1 s, and then smoothing the path with a 21- sample boxcar window filter (400 ms; 10 samples on each side). Spike sorting was performed offline using TINT cluster-cutting software and Klustakwik automated clustering tool. The resulting clusters were further refined manually and validated using autocorrelation and cross-correlation functions as additional separation tools. Quantitative measurements of cluster quality was subsequently performed, yielding isolation distances in Mahalanobis space (Schmitzer-Torbert et al., 2005).

The place cells were separated from inhibitory interneurons based on the spike width (> 300μs) and firing rate (< 30Hz). To ensure that we recorded from the same place cell across sessions, we confirmed that the properties such as autocorrelation, waveform, firing rate and firing location were similar in both sessions. The inhibitory interneurons were easily identified by their high frequency of firing with narrow waveform width and place nonspecific firing. Each sorted place cell was visualized by plotting its firing rate on top of an animal's walking path, with heat map colors ranging from blue (little or no firing) to red (high firing rate). A normalized firing rate map was obtained by dividing the spiking activity with the animal's position at a particular place. Firing rate maps were

smoothed with a filter such that 1 cm equaled 2 pixels. Peak firing was the maximum amount of firing by a cell in a particular session and average firing was calculated by dividing total spikes with total time in a session. Place field size was measured as in previous studies (Muller et al., 1987). Briefly, we calculated the number of pixels inside the enclosure where place cells fired normalized with the number of pixels the mice visited. Only the top 80% of the firing peak with at least 8 contiguous pixels was used and defined as the place field. Only the largest place field was used for place field analysis. Spatial coherence estimates smoothness of a place field. It was calculated by correlating the firing rate in each pixel with firing rates averaged with its neighboring 8 pixels. It measures the extent to which the firing rate in a pixel is predicted by the rates in its neighbors (Muller and Kubie, 1989). Abrupt changes in firing rates of neighboring pixels make the placefields incoherent. Spatial information content is a measure used to predict the location of an animal from the firing of a cell. Information content was calculated using Skaggs' formula (Markus et al., 1994; Skaggs et al., 1993) and measures the amount of information carried by a single spike about the location of the animal and is expressed as bits per spike:

$$Spatial\ information\ content = \sum Pi\left(\frac{Ri}{R}\right) log2\left(\frac{Ri}{R}\right)$$

where i is the bin/pixel number, Pi is the probability for occupancy of bin i, Ri is the mean firing rate for bin/pixel i and R is the overall firing mean rate. Spatial coherence and information content from session 1 were compared with measures from session 2. The reproducibility or stability of place fields is a good measure of animal's memory of space across time. It was calculated by performing a Pearson's product moment correlation on

two firing map fields across two consecutive sessions. Only regions covered by the animal in both sessions were compared and analyzed. The correlation formula is given by:

$$r = \frac{1}{n-1} \sum_{i=1}^{n} \left[\left(\frac{Xi - \bar{X}}{\sigma x} \right) \left(\frac{Yi - \bar{Y}}{\sigma y} \right) \right]$$

where $\frac{Xi - \bar{X}}{\sigma x}, \bar{X}$ and σx are the standard score, sample mean, and sample standard deviation of data X, respectively.

Histology

To determine the exact position of the tetrodes in the brain, mice were anesthetized with an overdose of 0.5 ml ketamine and xylazine solution (100 mg/kg and 10 mg/kg, respectively) and perfused with 4% PFA solution, following which the tetrodes were moved up and the mice decapitated. The brain was gently removed and stored in 4% PFA solution for 24 hr. It was then placed in a 30% sucrose solution for 48–72 hr and was coronally sliced in 30 μm thick sections using a cryostat. The sections were stained with cresyl violet and mounted onto a slide. The brain sections were viewed under a light microscope and digital pictures of the slices acquired. The tips of the tetrodes were identified visually and marked with red arrows.

SUPPLEMENTAL REFERENCES

Alamed, J., Wilcock, D.M., Diamond, D.M., Gordon, M.N., and Morgan, D. (2006). Two-day radial-arm water maze learning and memory task; robust resolution of amyloid-related memory deficits in transgenic mice. Nature protocols *1*, 1671-1679.

Barrett, J.C., Fry, B., Maller, J., and Daly, M.J. (2005). Haploview: analysis and visualization of LD and haplotype maps. Bioinformatics *21*, 263-265.

Hussaini, S.A., Kempadoo, K.A., Thuault, S.J., Siegelbaum, S.A., and Kandel, E.R. (2011). Increased size and stability of CA1 and CA3 place fields in HCN1 knockout mice. Neuron *72*, 643-653.

Markus, E.J., Barnes, C.A., Mcnaughton, B.L., Gladden, V.L., and Skaggs, W.E. (1994). Spatial Information-Content and Reliability of Hippocampal Ca1 Neurons - Effects of Visual Input. Hippocampus *4*, 410-421.

Martin, S.B., Dowling, A.L.S., Lianekhammy, J., Lott, I.T., Doran, E., Murphy, M.P., Beckett, T.L., Schmitt, F.A., and Head, E. (2014). Synaptophysin and Synaptojanin-1 in Down Syndrome are Differentially Affected by Alzheimer's Disease. J Alzheimers Dis *42*, 767-775.

McIntire, L.B., Berman, D.E., Myaeng, J., Staniszewski, A., Arancio, O., Di Paolo, G., and Kim, T.W. (2012). Reduction of synaptojanin 1 ameliorates synaptic and behavioral impairments in a mouse model of Alzheimer's disease. The Journal of neuroscience : the official journal of the Society for Neuroscience *32*, 15271-15276.

Muller, R.U., and Kubie, J.L. (1989). The Firing of Hippocampal Place Cells Predicts the Future Position of Freely Moving Rats. Journal of Neuroscience *9*, 4101-4110.

Muller, R.U., Kubie, J.L., and Ranck, J.B., Jr. (1987). Spatial firing patterns of hippocampal complex-spike cells in a fixed environment. The Journal of neuroscience : the official journal of the Society for Neuroscience *7*, 1935-1950.

Ongen, H., Buil, A., Brown, A.A., Dermitzakis, E.T., and Delaneau, O. (2016). Fast and efficient QTL mapper for thousands of molecular phenotypes. Bioinformatics *32*, 1479-1485.

Schmitzer-Torbert, N., Jackson, J., Henze, D., Harris, K., and Redish, A.D. (2005). Quantitative measures of cluster quality for use in extracellular recordings. Neuroscience *131*, 1-11.

Skaggs, W.E., McNaughton, B.L., Gothard, K.M., and Markus, E.J. (1993). An information-theoretic approach to deciphering the hippocampal code. Advances in Neural Processing Systems *5*, 1030-1037.

Stegle, O., Parts, L., Piipari, M., Winn, J., and Durbin, R. (2012). Using probabilistic estimation of expression residuals (PEER) to obtain increased power and interpretability of gene expression analyses. Nature protocols *7*, 500-507.